

INFIMED-FOUNDATION: PIONEERING ADVANCED MULTIMODAL MEDICAL MODELS WITH COMPUTE-EFFICIENT PRE-TRAINING AND MULTI-STAGE FINE-TUNING

Guanghao Zhu¹, Zhitian Hou^{2,3}, Zeyu Liu¹, Zhijie Sang³, Congkai Xie³, Hongxia Yang^{1,3*}

¹The Hong Kong Polytechnic University

²Sun Yat-sen University

³InfiX.ai

ABSTRACT

Multimodal large language models (MLLMs) have shown remarkable potential in various domains, yet their application in the medical field is hindered by several challenges. General-purpose MLLMs often lack the specialized knowledge required for medical tasks, leading to uncertain or hallucinatory responses. Knowledge distillation from advanced models struggles to capture domain-specific expertise in radiology and pharmacology. Additionally, the computational cost of continual pretraining with large-scale medical data poses significant efficiency challenges. To address these issues, we propose InfiMed-Foundation-1.7B and InfiMed-Foundation-4B, two medical-specific MLLMs designed to deliver state-of-the-art performance in medical applications. We combined high-quality general-purpose and medical multimodal data and proposed a novel five-dimensional quality assessment framework to curate high-quality multimodal medical datasets. We employ low-to-high image resolution and multimodal sequence packing to enhance training efficiency, enabling the integration of extensive medical data. Furthermore, a three-stage supervised fine-tuning process ensures effective knowledge extraction for complex medical tasks. Evaluated on the MedEvalKit framework, InfiMed-Foundation-1.7B outperforms Qwen2.5VL-3B, while InfiMed-Foundation-4B surpasses HuatuoGPT-V-7B and MedGemma-27B-IT, demonstrating superior performance in medical visual question answering and diagnostic tasks. By addressing key challenges in data quality, training efficiency, and domain-specific knowledge extraction, our work paves the way for more reliable and effective AI-driven solutions in healthcare. InfiMed-Foundation-4B model is available at InfiMed-Foundation-4B.

1 INTRODUCTION

In recent years, multimodal large language models (MLLMs) have demonstrated remarkable capabilities across various domains (Hurst et al., 2024; Team et al., 2025a; Zhu et al., 2025), achieving near-expert-level performance in tasks such as visual question answering (VQA), image captioning, and text generation. However, general-purpose MLLMs often lack the specialized knowledge required to address domain-specific challenges, particularly in the medical field (Lee et al., 2023). When tasked with medical queries, these models frequently produce uncertain or even hallucinatory responses (Li et al., 2023; Chen et al., 2024b), highlighting the need for domain-specific adaptations. The medical domain demands a high level of precision, reliability, and domain expertise, as inaccurate outputs can have significant consequences in clinical settings.

Recent efforts have focused on integrating medical multimodal data with general-purpose MLLMs to develop medical-specific models (Hyland et al., 2023; Team et al., 2025b). For instance, Lingshu (Team et al., 2025b) utilized a diverse set of open-source medical data, general-purpose data, and

*Corresponding author: hongxia.yang@polyu.edu.hk

high-quality synthetic medical data to train a model that achieved promising results across various medical evaluation benchmarks. These advancements underscore the potential of tailored MLLMs in tasks such as medical VQA and report generation. Despite these achievements, existing medical MLLMs face several challenges that limit their effectiveness and scalability. Firstly, many medical MLLMs rely on knowledge distillation from advanced general-purpose models (Hurst et al., 2024; Jaech et al., 2024) to curate training data. While effective in some contexts, this approach struggles to capture the extensive domain-specific expertise required for fields such as radiology, pharmacology, and pathology. Secondly, the absence of supervision by medical professionals during the distillation process consequently elevates the risk of generating model hallucinations. Thirdly, to inject comprehensive medical knowledge through continual pretraining, large-scale high-quality medical data is essential. However, processing such data is computationally expensive, necessitating strategies to enhance pretraining efficiency.

In this work, we propose InfiMed-Foundation-1.7B and InfiMed-Foundation-4B, two medical-specific MLLMs that achieve state-of-the-art performance across multiple medical benchmarks. To address the aforementioned challenges, we curated a high-quality multimodal medical dataset, combining carefully selected medical data with general-purpose multimodal data. In collaboration with medical professionals, we developed a novel five-dimensional quality assessment framework to ensure the reliability and relevance of the training data. During continual pretraining, we optimized computational efficiency by reducing the number of image patches to 144 and introducing multimodal sequence packing, which allowed us to incorporate a larger volume of medical data. Furthermore, we designed a three-stage supervised fine-tuning (SFT) process, comprising general instruction following, medical instruction following, and cross-distribution instruction adaptation. This structured approach enables our models to progressively acquire the ability to address complex medical tasks effectively.

We evaluated our models using the MedEvalKit framework (Team et al., 2025b), a comprehensive suite of medical benchmarks. Experimental results demonstrate that InfiMed-Foundation-1.7B outperforms the Qwen2.5VL-3B model (Bai et al., 2025), while InfiMed-Foundation-4B surpasses both the HuatuoGPT-V-7B (Chen et al., 2024b) and MedGemma-27B-IT (Sellergren et al., 2025) models. Through ablation studies, we validated the critical role of our multi-stage SFT strategy. Additionally, case studies in medical VQA and diagnostic tasks highlight the superior performance of our models, showcasing their potential to assist clinicians in real-world scenarios.

Our contributions can be summarized as follows:

- **Data Curation:** We introduce a five-dimensional quality assessment framework, developed in collaboration with medical professionals, to select high-quality medical datasets, ensuring robustness and reliability in training.
- **Training Efficiency:** We enhance pretraining efficiency by adopting multimodal sequence packing and reducing image patch counts, enabling the incorporation of extensive medical data while minimizing computational costs.
- **Performance:** Our InfiMed-Foundation models achieve outstanding results across multiple medical evaluation benchmarks, setting a new standard for medical-specific MLLMs.

2 RELATED WORK

Medical-Specific Multimodal Models Medical-specific MLLMs have gained traction for tasks such as clinical reasoning, medical VQA, and report generation. LLaVA-Med (Li et al., 2023) pioneered this domain by utilizing large-scale biomedical image-text pairs from PubMed Central for concept alignment, enabling the model to learn domain-specific visual vocabulary, followed by instruction tuning with GPT-4-generated data. However, the low quality of PubMed data often leads to hallucinations and weak reasoning capabilities, as the instruction data relies solely on textual captions and contexts without leveraging biomedical images. In contrast, HuatuoGPT-Vision (Chen et al., 2024b) employs GPT-4V, a multimodal model capable of processing both images and text, to denoise PubMed data and create the high-quality PubMedVision dataset for SFT, improving performance in medical VQA. MedGemma (Sellergren et al., 2025) adopts a multi-stage training pipeline. First, the vision encoder is enhanced using medical image-text pairs. Subsequently, the language model undergoes continual pretraining and is then re-adapted with the vision encoder. Finally, the model is refined through distillation and reinforcement learning. Despite these advances, existing models of-

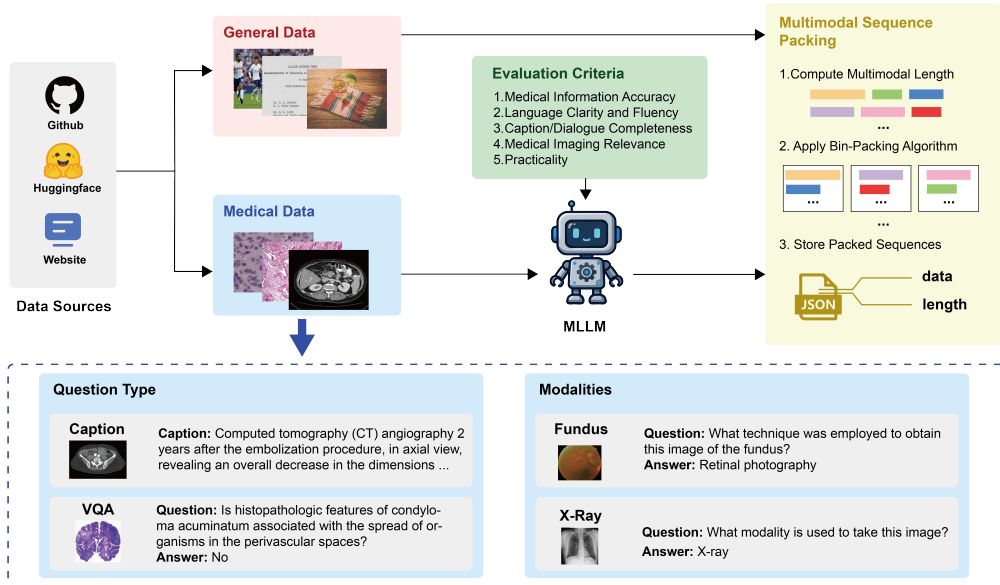


Figure 1: The pipeline of our dataset curation.

ten lack robust data quality control and professional supervision, limiting their reliability in clinical settings. Our InfiMed-Foundation models address these issues by combining high-quality general and medical multimodal data. A novel five-dimensional quality assessment framework, developed with medical professionals, ensures robust performance.

Efficient Training Strategies for Multimodal Models MLLM pretraining aims to align different modalities in a shared embedding space, requiring large-scale image-text pair datasets. Many approaches train only the vision-language projector to mitigate catastrophic forgetting and reduce computational costs while freezing the vision encoder and language model (Jin et al., 2024). However, TinyLLaVA (Zhou et al., 2024) notes that training only the projector may lead to suboptimal alignment in small-scale LLMs, proposing partial unfreezing of the vision encoder and LLM to improve modality alignment. Similarly, VILA (Lin et al., 2024) demonstrates that unfreezing LLM parameters during pretraining is essential for inheriting in-context learning capabilities, which are critical for personalized medical recommendations in clinical settings. To further enhance efficiency, Idefics2 (Laurençon et al., 2024) employs a perceiver resampler to reduce visual token counts. It adopts a two-stage pretraining approach, using lower image resolutions in the initial stage to accelerate basic alignment. Inspired by these works, our InfiMed-Foundation models unfreeze both the projector and LLM parameters during pretraining and introduce multimodal sequence packing with a reduced image patch count of 144, significantly improving computational efficiency while enabling the integration of extensive medical data.

3 DATASET CURATION

To train our proposed InfiMed-Foundation series models, we curated a large-scale, heterogeneous dataset comprising both medical and general-domain multimodal data. The pipeline of our dataset curation is shown in Figure 1. The medical dataset covers diverse modalities, body parts, question types, and multiple languages. To improve the model’s generalization and linguistic capabilities, we further curated a large-scale general-domain dataset encompassing diverse real-world scenarios. To ensure data quality, we developed an evaluation pipeline based on LLMs, which was used to assess and filter the collected datasets. An overview of all collected datasets is provided in Table 1.

3.1 DATA COLLECTION

Medical Data To build a high-quality medical dataset for training our InfiMed-Foundation models, we collected and aggregated a range of multimodal medical datasets from public sources, which include image-text pairs. Moreover, we divided them into two categories: caption and instruction. The collected multimodal medical data span various modalities (e.g., pathology, microscopy, and

Table 1: Overview of Training datasets.

Type of Data	Collected Datasets
General Caption Data	DataComp (Gadre et al., 2023), CCS (Li et al., 2022)
General Interleaved Data	OBELICS (Laurençon et al., 2023), mmc4 (Zhu et al., 2023)
General Instruction Data	Mammoth-VL (Guo et al., 2024)
Medical Caption Data	IU-Xray (Chen et al., 2020), LLaVA-Med (Li et al., 2023), LLaVA-Med-60K-IM-text (Kang, 2024), Medtrinity-25M (Xie et al., 2025), MedPix-2.0 (Siragusa et al., 2025), PMC-OA (Lin et al., 2023), PubMedVision (Chen et al., 2024a), ROCO (Pelka et al., 2018), ROCov2 (Rückert et al., 2024)
Medical Instruction Data	LLaVA-Med (Li et al., 2023), Path-VQA (He et al., 2020), PMC-VQA (Zhang et al., 2023), PubMedVision (Chen et al., 2024a), SLAKE (Liu et al., 2021), VQA-Med-2019 (Ben Abacha et al., 2019), VQA-RAD (Lau et al., 2018)

CT), body parts (e.g., head, neck, and chest), question types (e.g., open-ended, closed-ended, and multiple-choice), and multiple languages (e.g., English and Chinese).

General Data To enable the multimodal large language model to achieve strong multimodal understanding and visual reasoning capabilities, it is necessary to conduct continual pretraining on large-scale image-text caption datasets and interleaved datasets. For general data collection, we followed the highly open-source Open-Qwen2VL (Wang et al., 2025). Specifically, for general caption data, we used two subsets of DataComp-Medium-128M (Gadre et al., 2023), filtered by Data-Filtering-Network (DFN) (Fang et al., 2023) and MLM-Filter (Wang et al., 2024), respectively. Additionally, we incorporated high-quality caption data from the BLIP (Li et al., 2022), which was filtered from a combination of three web datasets: CC3M (Changpinyo et al., 2021), CC12M (Changpinyo et al., 2021), and SBU (Ordonez et al., 2011) (CCS). For general interleaved data, we employed high-quality subsets of the OBELICS dataset (Laurençon et al., 2023) and the MMC4 dataset (Zhu et al., 2023) to enhance the multimodal in-context learning ability. And we utilized the MAMMOTH-VL-10M (Guo et al., 2024) to bolster the model’s instruction-following and reasoning capabilities.

3.2 DATA EVALUATION

We performed quality control on medical data using both LLM-based and manual inspection. To evaluate data quality, we randomly sampled 500 samples from each dataset and conducted a detailed evaluation. We collaborated with a group of medical professionals to define five evaluation criteria:

1. **Medical Information Accuracy:** Assess how medically accurate and clinically appropriate the information in the sample is.
2. **Language Clarity and Fluency:** Assess how well the content is communicated in natural, readable, and professional language.
3. **Caption/Dialogue Completeness:** Assess whether the caption/dialogue directly, sufficiently, and contextually addresses the input question or medical concern.
4. **Medical Imaging Relevance:** For samples that include an image, assess whether the image clearly supports or corresponds to the associated text.
5. **Practicality:** Assess how useful the data sample is for real-world medical applications, such as clinical decision support or patient communication.

Each dimension was rated on a scale of 1 to 5. Detailed scoring guidelines are provided in Appendix A.2. We employed GPT-o3 as an automated evaluator to rate the sampled data according to the above criteria. The results guided our filtering process and informed our overall data quality assessment. After our quality assessment, we excluded some datasets, including IU-Xray, MedPix-2.0, PMC-OA, and VQA-Med-2019.

3.3 MULTIMODAL SEQUENCE PACKING

Owing to the variable sequence lengths inherent in multimodal data, direct training often necessitates padding all samples to a uniform maximum length. This practice introduces a substantial number of padding tokens, resulting in significant computational inefficiency. To address this issue, we employ a multimodal sequence-packing strategy during continuous pretraining. This method reorganizes multiple multimodal samples into consolidated sequences with total lengths approaching the model’s maximum context window of 4,096 tokens.

The multimodal sequence packing procedure consists of the following three steps:

1. **Compute Multimodal Length:** The token length of each multimodal sample, which incorporates both visual and textual elements, is calculated.
2. **Apply Bin-Packing Algorithm:** Samples are sorted in descending order of their lengths and subsequently packed into bins using the First-Fit-Decreasing (FFD) bin packing algorithm (Johnson, 1973). The objective is to aggregate samples into bins such that the cumulative length of each bin is as close as possible to, but does not exceed, 4,096 tokens.
3. **Store Packed Sequences:** Each consolidated bin of packed sequences is saved into a JSON file. The structure of the file is organized as a dictionary containing the following two key fields:
 - "data": A list of the regrouped samples. Each sample within the list is a dictionary itself, containing the Base64-encoded image data, the corresponding text, and other metadata.
 - "lengths": A list of integers that records the original multimodal sequence length of each constituent sample within the bin.

4 MODEL TRAINING

InfiMed-Foundation models consist of three key components: a LLM, a vision encoder, and a lightweight MLP-based visual projector. We adopt this architecture with Qwen3-Instruct series LLMs (Yang et al., 2025), SigLIP-SO-400M Vision Encoder (Tang et al., 2002), and Adaptive Average-Pooling Visual Projector (Yao et al., 2024). Specifically, the visual projector consists of an Adaptive Average-Pooling layer followed by a two-layer MLP. The adaptive pooling layer allows us to flexibly rescale the fixed output of 729 visual patches from the SigLIP encoder to any desired number of visual tokens. During pretraining, we downsample the visual representation to 144 visual tokens per image to reduce computational cost and encourage global abstraction. In the supervised fine-tuning (SFT) stage, we revert to the full 729 patches resolution to capture more detailed visual cues. This design offers a good trade-off between efficiency and flexibility, allowing the model to adaptively balance global and local visual features across different training phases.

4.1 TRAINING RECIPE

During both the pretraining and supervised fine-tuning (SFT) stages, we freeze the parameters of the vision encoder to reduce computational cost. Only the LLM and the projector are trainable.

In the pretraining stage, we train the model on a large corpus comprising general-domain multimodal samples ($\sim 25\text{B}$ tokens) and medical samples ($\sim 5\text{B}$ tokens). And inspired by Allen-Zhu & Li (2024), we adopt Instruct series models instead of base series models for pretraining, aiming to enhance the model’s contextual understanding and adaptation efficiency in the subsequent alignment stages.

Inspired by the multi-stage alignment strategy proposed in Lingshu (Team et al., 2025b), we design a three-stage SFT pipeline to progressively inject and align different capabilities into the model as illustrated in Figure 2. The three stages in our pipeline are: 1) General Instruction Following: Enhancing the model’s ability to follow general-purpose instructions in diverse contexts. 2) Medical Instruction Following: Fine-tuning the model for medical-domain tasks that require domain-specific reasoning and understanding. 3) Cross-distribution Instruction Adaptation: To ensure generalization across heterogeneous data sources, we apply down-sampling to each dataset, enforcing inter-dataset balance. This prevents overfitting to high-resource instruction types and encourages the model to adapt to a wide range of data distributions. The details of the data mixture for different training stages are provided in Appendix A.3.

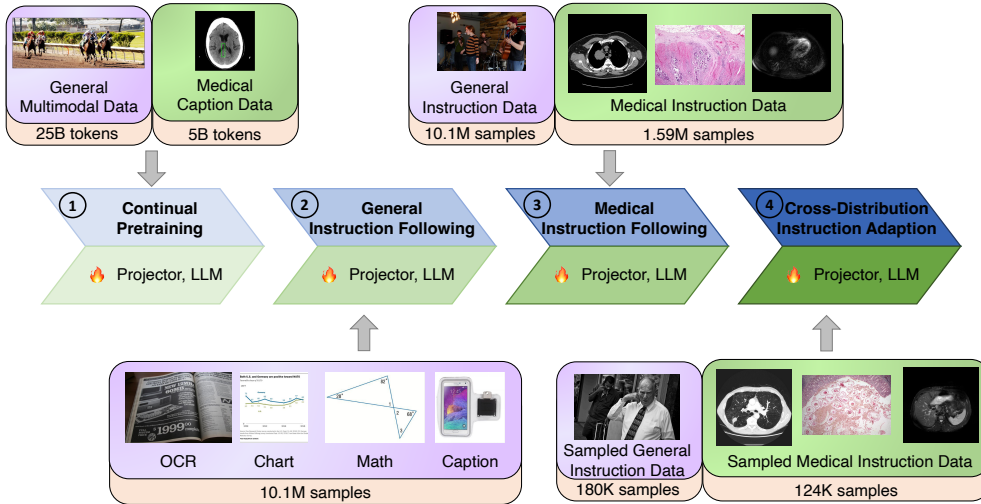


Figure 2: The training pipeline of InfiMed-Foundation models, which consists of four stages: continual pretraining, general instruction following, medical instruction following, and cross-distribution instruction adaption.

4.1.1 COMPUTE-EFFICIENT PRETRAINING

The primary objective of pretraining multimodal medical models is to achieve robust alignment between image and text modalities while injecting domain-specific medical knowledge into the model. This alignment enhances the model’s ability to understand medical visual data, laying a critical foundation for subsequent knowledge extraction in tasks such as medical VQA and diagnostic support (Li et al., 2023; Chen et al., 2024b). However, pretraining large-scale multimodal models, especially with high-resolution medical images and diverse text data, is computationally intensive.

In our pretraining phase, we freeze the vision encoder to preserve its pretrained feature extraction capabilities, while updating the parameters of the LLM and the projector. Our pretraining dataset comprises high-quality general-purpose multimodal data and medical image-text pairs curated using our five-dimensional quality assessment framework. To enhance the efficiency of pretraining, we employ multimodal sequence packing, a strategy that concatenates multimodal data of varying lengths into sequences approaching a maximum length of 4096 tokens. This approach maximizes computational resource utilization by minimizing padding and ensuring dense data processing. Additionally, we implement adaptive average-pooling to reduce the number of tokens representing images to 144. This reduction mitigates computational overhead while preserving essential visual features.

4.1.2 GENERAL INSTRUCTION FOLLOWING

The first stage of our SFT pipeline, termed General Instruction Following, aims to endow the InfiMed-Foundation models with robust multimodal reasoning and instruction-following capabilities, establishing a strong foundation for subsequent medical domain adaptation. Unlike medical-specific fine-tuning, which focuses on domain knowledge, this stage emphasizes general multimodal understanding, ensuring the model can handle complex reasoning tasks before specializing in medical applications. We leverage the MAMmoTH-VL-10M dataset (Guo et al., 2024), a large-scale multimodal instruction-tuning dataset designed to foster reasoning-intensive capabilities.

The MAMmoTH-VL-10M dataset is specifically curated to address the limitations of traditional instruction datasets, which often focus on simple VQA tasks with phrase-based responses lacking detailed reasoning processes. To construct MAMmoTH-VL-10M, data sources underwent manual screening to categorize based on the information density of responses. Subsequently, a combination of MLLMs and LLMs was used to rewrite responses, generating detailed rationales. Finally, an MLLM-based filtering step ensured logical consistency and reliability of the rationales. By training

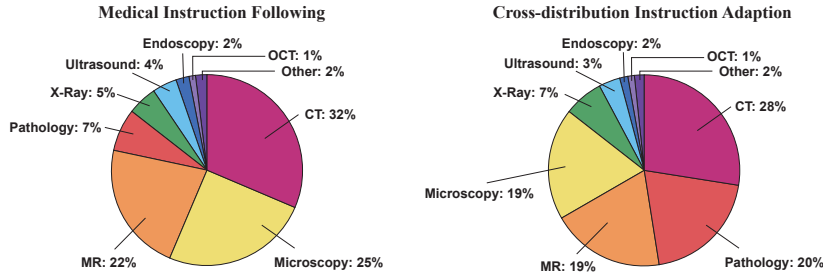


Figure 3: The modality distribution of the dataset in the Medical Instruction Following stage and the Cross-distribution Instruction Adaption stage.

on MAMmoTH-VL-10M’s detailed rationales, our models develop enhanced reasoning abilities, which are critical for subsequent medical-specific fine-tuning stages.

4.1.3 MEDICAL INSTRUCTION FOLLOWING

To equip the model with medical question-answering capabilities, the second stage of our fine-tuning pipeline is dedicated to medical instruction tuning. In this stage, the model is trained on a collection of high-quality medical VQA datasets that have passed the rigorous data quality assessment detailed in Section 3.2. These datasets span a diverse range of medical subdomains, including clinical diagnostics, radiological interpretation, and pathological analysis, each requiring varying degrees of domain-specific reasoning and precision.

To avoid catastrophic forgetting of general capabilities acquired in the first stage, we incorporate general instruction-following data into this phase. This joint training strategy allows the model to retain its general multimodal abilities while enhancing its understanding of medical knowledge. Importantly, this approach prevents the model from overfitting to narrow medical domains and promotes better generalization across both general-domain and medical-domain tasks.

4.1.4 CROSS-DISTRIBUTION INSTRUCTION ADAPTION

Naively fine-tuning on a mixture of medical VQA datasets in a single stage risks overfitting to high-resource datasets, as they disproportionately influence the training objective. This imbalance undermines the model’s generalization to low-resource tasks and diverse instruction distributions. To address this, the third stage introduces cross-distribution instruction adaptation. In this stage, we construct mixed instruction datasets by sampling from multiple datasets across both general and medical domains. Furthermore, we also balance the number of samples between medical and general instruction datasets to prevent distributional bias during training. To ensure inter-dataset balance, we down-sample large datasets to bring all sources to a similar scale, avoiding domination by high-resource datasets. The modality distribution of the dataset in the Medical Instruction Following stage and the Cross-distribution Instruction Adaption stage is shown in Figure 3.

Importantly, this stage retains the same architectural configuration and optimization settings as previous stages. This approach preserves training stability while enhancing the model’s ability to generalize across heterogeneous datasets and instruction formats.

5 EXPERIMENTS

To comprehensively evaluate our model, InfiMed-Foundation, we compare its performance against a diverse set of baseline models on various medical benchmarks. These baselines include proprietary and open-source models, with the latter encompassing general-purpose and medical-specific models. Specifically, our evaluation includes the following models: **Proprietary Models:** GPT-5, GPT-5-mini, GPT-5-nano, GPT-4.1 (OpenAI, 2025), Claude Sonnet 4 (Anthropic, 2025), Gemini-2.5-Flash (Comanici et al., 2025). **General Open-source Models:** Qwen2.5-VL-Instruct (Bai et al., 2025), InternVL3 (Zhu et al., 2025). **Medical Open-source Models:** MedGemma (Sellergren et al., 2025), LLaVA-Med (Li et al., 2023), HuatuoGPT-V (Chen et al., 2024b), Lingshu (Team et al., 2025b), BioMediX2 (Mullappilly et al., 2024).

To ensure a fair comparison, all models are evaluated using MedEvalKit (Team et al., 2025b), a systematic evaluation framework. This framework assesses performance across mainstream medical benchmarks, including multiple-choice questions, open-ended questions, and other task formats.

5.1 EVALUATION BENCHMARK

To comprehensively evaluate the performance of medical MLLMs, we utilized a diverse set of medical benchmark datasets. These benchmarks include multiple-choice, open-ended, and closed-ended questions, covering datasets such as the Health & Medical subset of MMMU (Yue et al., 2024), VQA-RAD (Lau et al., 2018), SLAKE (Liu et al., 2021), PathVQA (He et al., 2020), PMC-VQA (Zhang et al., 2023), the open-source portion of OmniMedVQA (Hu et al., 2024), and the multimodal subset of MedXpertQA (Zuo et al., 2025). These datasets encompass various medical imaging modalities, including CT scans, dermoscopy, X-rays, and microscopy images. This variety enables a robust assessment of the model’s ability to process and interpret diverse medical visual data, ensuring a comprehensive evaluation of its medical reasoning and multimodal understanding capabilities. Our evaluation framework and implementation details can be found in the Appendix A.4 and Appendix A.5.

5.2 MAIN RESULTS

Table 2 presents a comprehensive comparison of our proposed models, InfiMed-Foundation-1.7B and InfiMed-Foundation-4B, against both proprietary and open-source MLLMs across seven representative medical benchmarks. The final column shows the macro-average across all benchmarks.

InfiMed-Foundation-4B achieves an average accuracy of 56.4%, outperforming all general and medical open-source MLLMs of comparable scale and closing the gap with several strong proprietary systems. Notably, InfiMed-Foundation-4B exceeds MedGemma-27B-IT (+1.0%) and HuatuoGPT-V-7B (+2.2%) despite having fewer parameters, demonstrating superior parameter efficiency. Compared to LLaVA-Med-7B, a widely-used baseline, InfiMed-Foundation-4B shows a substantial +18.6% gain on average performance. Among individual benchmarks, InfiMed-Foundation-4B achieves particularly strong results on PathVQA (63.4%), outperforming all open-source medical baselines, and on SLAKE (77.7%), where it ranks second only to Lingshu-7B (83.1%). While performance on MedXVQA remains modest (21.9%), this is consistent with trends across other open models and highlights the dataset’s unique challenges. Interestingly, InfiMed-Foundation-1.7B maintains competitive performance across most datasets despite its smaller scale, indicating that our architecture and training approach are robust across sizes. For instance, it surpasses BioMediX2-8B by +6.2% on average, despite having one-fifth the parameter count. We include a set of comparative case studies of our InfiMed-Foundation-4B model versus Qwen2.5-VL-7B in the Appendix A.6.

While proprietary models like GPT-5 (70.0%) and Gemini-2.5-Flash (65.1%) still lead in overall accuracy, our results demonstrate that InfiMed-Foundation-4B achieves state-of-the-art performance among open-source medical MLLMs, and narrows the performance gap with closed models significantly, especially considering compute and scale limitations.

5.3 ABLATION STUDY

To investigate the contributions of each stage in the SFT process outlined in Section 4.1, we conducted an ablation study by selectively applying the three SFT stages: General Instruction Following (Stage 1), Medical Instruction Following (Stage 2), and Cross-distribution Instruction Adaptation (Stage 3). This study aims to quantify the impact of each stage on the performance of our multimodal medical large language model across various benchmarks. The results are summarized in Table 3.

Each SFT stage contributes differently to the model’s performance across various tasks. When omitting Stage 2 (Medical Instruction Following) and performing only Stage 1 (General Instruction Following), we observe a significant performance drop on benchmarks such as SLAKE, PMC-VQA, and OmniMedVQA. This underscores the importance of incorporating high-quality medical VQA datasets during Stage 2, which enhances the model’s ability to address domain-specific medical queries effectively.

Table 2: Results of comparison of InfiMed with other MLLMs on medical multimodal benchmarks. Note that OMVQA and MedXQA indicate OmniMedVQA and MedXpertQA-Multimodal benchmarks, respectively. Models colored in gray denote our InfiMed.

Model	MMM-U-Med	VQA-RAD	SLAKE	PathVQA	PMC-VQA	OMVQA	MedXVQA	Avg.
Proprietary Models								
GPT-5	83.6	67.8	78.1	52.8	60.0	76.4	71.0	70.0
GPT-5-mini	80.5	66.3	76.1	52.4	57.6	70.9	60.1	66.3
GPT-5-nano	74.1	55.4	69.3	45.4	51.3	66.5	45.1	58.2
GPT-4.1	75.2	65.0	72.2	55.5	55.2	75.5	45.2	63.4
Claude Sonnet 4	74.6	67.6	70.6	54.2	54.4	65.5	43.3	61.5
Gemini-2.5-Flash	76.9	68.5	75.8	55.4	55.4	71.0	52.8	65.1
General Open-source Models								
Qwen2.5VL-3B	51.3	56.8	63.2	37.1	50.6	64.5	20.7	49.2
Qwen2.5VL-7B	50.6	64.5	67.2	44.1	51.9	63.6	22.3	52.0
InternVL3-8B	59.2	65.4	72.8	48.6	53.8	79.1	22.4	57.3
Medical Open-source Models								
MedGemma-4B-IT	43.7	49.9	76.4	48.8	49.9	69.8	22.3	51.5
LLaVA-Med-7B	29.3	53.7	48.0	38.8	30.5	44.3	20.3	37.8
HuatuoGPT-V-7B	47.3	67.0	67.8	48.0	53.3	74.2	21.6	54.2
Lingshu-7B	54.0	67.9	83.1	61.9	56.3	82.9	26.7	61.8
BioMediX2-8B	39.8	49.2	57.7	37.0	43.5	63.3	21.8	44.6
MedGemma-27B-IT	56.2	62.3	74.9	44.4	49.5	66.3	33.9	55.4
InfiMed-Foundation-1.7B	34.7	56.3	75.3	60.7	48.1	58.9	21.8	50.8
InfiMed-Foundation-4B	43.3	57.9	77.7	63.4	56.6	76.8	21.9	56.4

Table 3: Ablation study results for SFT stages on medical multimodal benchmarks.

SFT Stage			Medical Benchmarks							
Stage 1	Stage 2	Stage 3	MMM-U-Med	VQA-RAD	SLAKE	PathVQA	PMC-VQA	OMVQA	MedXVQA	Avg.
✓			42.7	53.7	62.3	51.6	54.2	71.8	21.9	51.2
✓	✓		41.3	53.0	73.1	50.5	58.8	77.8	19.0	53.4
✓		✓	41.3	53.4	76.0	61.7	51.0	72.0	21.3	53.8
✓	✓	✓	43.3	57.9	77.7	63.4	56.6	76.8	21.9	56.4

In contrast, the inclusion of Stage 3 (Cross-distribution Instruction Adaptation) leads to substantial performance improvements, particularly on VQA-RAD, SLAKE, and PathVQA, with accuracy gains of 4.9%, 4.6%, and 12.9%, respectively, over the configuration with only Stages 1 and 2. This indicates that Stage 3 effectively mitigates the risk of model domination by larger medical datasets, enabling better generalization across diverse data distributions. By adapting the model to handle cross-distribution variations, Stage 3 ensures robust performance on benchmarks with differing data characteristics, such as the radiologically focused VQA-RAD and the pathology-oriented PathVQA. Furthermore, when performing only Stages 1 and 3, we observe improved performance on SLAKE and PathVQA compared to the configuration with only Stages 1 and 2, with accuracy gains of 3.1%, and 11.2%, respectively. This improvement is attributed to Stage 3’s ability to mitigate the risk of model domination by larger medical datasets. However, this configuration results in a notable performance drop on PMC-VQA and OmniMedVQA, with accuracy reductions of 7.8% and 5.8%, respectively. These results highlight the necessity of including Stage 2 to leverage more medical-related data for maintaining robust performance. Therefore, the optimal configuration requires all three stages.

The ablation study demonstrates the complementary nature of the three stages: Stage 1 establishes a strong foundation in general instruction following, Stage 2 enhances medical domain expertise, and Stage 3 ensures adaptability to diverse data distributions. Together, these stages enable our model to achieve state-of-the-art performance in multimodal medical tasks.

6 CONCLUSION

In this work, we introduce InfiMed-Foundation-1.7B and InfiMed-Foundation-4B, two medical-specific multimodal large language models. We present a novel five-dimensional quality assessment framework developed with medical professionals to obtain a curated high-quality multimodal medical dataset. By optimizing pretraining efficiency with multimodal sequence packing and scaling

down image patches, we incorporated extensive medical data cost-effectively. Our three-stage supervised fine-tuning process enabled robust performance across complex medical tasks. Evaluations using the MedEvalKit framework showed that InfiMed-Foundation-1.7B outperforms Qwen2.5VL-3B, while InfiMed-Foundation-4B surpasses HuatuoGPT-V-7B and MedGemma-27B-IT, setting new standards for medical MLLMs. Ablation studies and case studies in medical VQA and diagnostics confirmed the critical role of our SFT strategy and data curation, highlighting the models' potential to assist clinicians. Our contributions in data curation, training efficiency, and performance pave the way for scalable medical AI, with future work aimed at optimizing the vision encoder and expanding data diversity to further enhance model capabilities.

REFERENCES

- Zeyuan Allen-Zhu and Yuanzhi Li. Physics of Language Models: Part 3.1, Knowledge Storage and Extraction. In *Proceedings of the 41st International Conference on Machine Learning, ICML '24*, July 2024. Full version available at <https://ssrn.com/abstract=5250633>.
- Anthropic. Introducing Claude 4. <https://www.anthropic.com/news/claude-4>, may 2025.
- Shuai Bai, Keqin Chen, Xuejing Liu, Jialin Wang, Wenbin Ge, Sibao Song, Kai Dang, Peng Wang, Shijie Wang, Jun Tang, Humen Zhong, Yuanzhi Zhu, Mingkun Yang, Zhaohai Li, Jianqiang Wan, Pengfei Wang, Wei Ding, Zheren Fu, Yiheng Xu, Jiabo Ye, Xi Zhang, Tianbao Xie, Zesen Cheng, Hang Zhang, Zhibo Yang, Haiyang Xu, and Junyang Lin. Qwen2.5-vl technical report, 2025. URL <https://arxiv.org/abs/2502.13923>.
- Asma Ben Abacha, Sadid A Hasan, Vivek V Datla, Dina Demner-Fushman, and Henning Müller. Vqa-med: Overview of the medical visual question answering task at imageclef 2019. In *Proceedings of CLEF (Conference and Labs of the Evaluation Forum) 2019 Working Notes*. 9-12 September 2019, 2019.
- Soravit Changpinyo, Piyush Sharma, Nan Ding, and Radu Soricut. Conceptual 12m: Pushing web-scale image-text pre-training to recognize long-tail visual concepts. In *Proceedings of the IEEE/CVF conference on computer vision and pattern recognition*, pp. 3558–3568, 2021.
- Junying Chen, Chi Gui, Ruyi Ouyang, Anningzhe Gao, Shunian Chen, Guiming Hardy Chen, Xidong Wang, Zhenyang Cai, Ke Ji, Xiang Wan, and Benyou Wang. Towards injecting medical visual knowledge into multimodal LLMs at scale. In Yaser Al-Onaizan, Mohit Bansal, and Yun-Nung Chen (eds.), *Proceedings of the 2024 Conference on Empirical Methods in Natural Language Processing*, pp. 7346–7370, Miami, Florida, USA, November 2024a. Association for Computational Linguistics. doi: 10.18653/v1/2024.emnlp-main.418. URL <https://aclanthology.org/2024.emnlp-main.418/>.
- Junying Chen, Chi Gui, Ruyi Ouyang, Anningzhe Gao, Shunian Chen, Guiming Hardy Chen, Xidong Wang, Ruifei Zhang, Zhenyang Cai, Ke Ji, et al. Huatuogpt-vision, towards injecting medical visual knowledge into multimodal llms at scale. *arXiv preprint arXiv:2406.19280*, 2024b.
- Zhihong Chen, Yan Song, Tsung-Hui Chang, and Xiang Wan. Generating radiology reports via memory-driven transformer. In *Proceedings of the 2020 Conference on Empirical Methods in Natural Language Processing*, November 2020.
- Gheorghe Comanici, Eric Bieber, Mike Schaekermann, Ice Pasupat, Noveen Sachdeva, Inderjit Dhillon, Marcel Blistein, Ori Ram, Dan Zhang, Evan Rosen, et al. Gemini 2.5: Pushing the frontier with advanced reasoning, multimodality, long context, and next generation agentic capabilities. *arXiv preprint arXiv:2507.06261*, 2025.
- Alex Fang, Albin Madappally Jose, Amit Jain, Ludwig Schmidt, Alexander Toshev, and Vaishaal Shankar. Data filtering networks. *arXiv preprint arXiv:2309.17425*, 2023.
- Samir Yitzhak Gadre, Gabriel Ilharco, Alex Fang, Jonathan Hayase, Georgios Smyrnis, Thao Nguyen, Ryan Marten, Mitchell Wortsman, Dhruva Ghosh, Jieyu Zhang, et al. Datacomp: In search of the next generation of multimodal datasets. *Advances in Neural Information Processing Systems*, 36:27092–27112, 2023.
- Jarvis Guo, Tuney Zheng, Yuelin Bai, Bo Li, Yubo Wang, King Zhu, Yizhi Li, Graham Neubig, Wenhu Chen, and Xiang Yue. Mammoth-vl: Eliciting multimodal reasoning with instruction tuning at scale. *arXiv preprint arXiv:2412.05237*, 2024.
- Xuehai He, Yichen Zhang, Luntian Mou, Eric Xing, and Pengtao Xie. Pathvqa: 30000+ questions for medical visual question answering, 2020. URL <https://arxiv.org/abs/2003.10286>.
- Yutao Hu, Tianbin Li, Quanfeng Lu, Wenqi Shao, Junjun He, Yu Qiao, and Ping Luo. Omnimedvqa: A new large-scale comprehensive evaluation benchmark for medical lvlm. In *Proceedings of the IEEE/CVF Conference on Computer Vision and Pattern Recognition*, pp. 22170–22183, 2024.

- Aaron Hurst, Adam Lerer, Adam P Goucher, Adam Perelman, Aditya Ramesh, Aidan Clark, AJ Ostrow, Akila Welihinda, Alan Hayes, Alec Radford, et al. Gpt-4o system card. *arXiv preprint arXiv:2410.21276*, 2024.
- Stephanie L Hyland, Shruthi Bannur, Kenza Bouzid, Daniel C Castro, Mercy Ranjit, Anton Schwaighofer, Fernando Pérez-García, Valentina Salvatelli, Shaury Srivastav, Anja Thieme, et al. Maira-1: A specialised large multimodal model for radiology report generation. *arXiv preprint arXiv:2311.13668*, 2023.
- Aaron Jaech, Adam Kalai, Adam Lerer, Adam Richardson, Ahmed El-Kishky, Aiden Low, Alec Helyar, Aleksander Madry, Alex Beutel, Alex Carney, et al. Openai o1 system card. *arXiv preprint arXiv:2412.16720*, 2024.
- Yizhang Jin, Jian Li, Yexin Liu, Tianjun Gu, Kai Wu, Zhengkai Jiang, Muyang He, Bo Zhao, Xin Tan, Zhenye Gan, et al. Efficient multimodal large language models: A survey. *arXiv preprint arXiv:2405.10739*, 2024.
- David S Johnson. *Near-optimal bin packing algorithms*. PhD thesis, Massachusetts Institute of Technology, 1973.
- Myeongkyun Kang. Llava-med-60k-im-text. <https://huggingface.co/datasets/myeongkyunkang/LLaVA-Med-60K-IM-text>, 2024.
- Woosuk Kwon, Zhuohan Li, Siyuan Zhuang, Ying Sheng, Lianmin Zheng, Cody Hao Yu, Joseph Gonzalez, Hao Zhang, and Ion Stoica. Efficient memory management for large language model serving with pagedattention. In *Proceedings of the 29th symposium on operating systems principles*, pp. 611–626, 2023.
- Jason J Lau, Soumya Gayen, Asma Ben Abacha, and Dina Demner-Fushman. A dataset of clinically generated visual questions and answers about radiology images. *Scientific data*, 5(1):1–10, 2018.
- Hugo Laurençon, Lucile Saulnier, Léo Tronchon, Stas Bekman, Amanpreet Singh, Anton Lozhkov, Thomas Wang, Siddharth Karamcheti, Alexander Rush, Douwe Kiela, et al. Obelics: An open web-scale filtered dataset of interleaved image-text documents. *Advances in Neural Information Processing Systems*, 36:71683–71702, 2023.
- Hugo Laurençon, Léo Tronchon, Matthieu Cord, and Victor Sanh. What matters when building vision-language models? *Advances in Neural Information Processing Systems*, 37:87874–87907, 2024.
- Peter Lee, Sebastien Bubeck, and Joseph Petro. Benefits, limits, and risks of gpt-4 as an ai chatbot for medicine. *New England Journal of Medicine*, 388(13):1233–1239, 2023.
- Chunyuan Li, Cliff Wong, Sheng Zhang, Naoto Usuyama, Haotian Liu, Jianwei Yang, Tristan Naumann, Hoifung Poon, and Jianfeng Gao. Llava-med: Training a large language-and-vision assistant for biomedicine in one day. *Advances in Neural Information Processing Systems*, 36:28541–28564, 2023.
- Junnan Li, Dongxu Li, Caiming Xiong, and Steven Hoi. Blip: Bootstrapping language-image pre-training for unified vision-language understanding and generation. In *International conference on machine learning*, pp. 12888–12900. PMLR, 2022.
- Ji Lin, Hongxu Yin, Wei Ping, Pavlo Molchanov, Mohammad Shoeybi, and Song Han. Vila: On pre-training for visual language models. In *Proceedings of the IEEE/CVF conference on computer vision and pattern recognition*, pp. 26689–26699, 2024.
- Weixiong Lin, Ziheng Zhao, Xiaoman Zhang, Chaoyi Wu, Ya Zhang, Yanfeng Wang, and Weidi Xie. Pmc-clip: Contrastive language-image pre-training using biomedical documents, 2023. URL <https://arxiv.org/abs/2303.07240>.
- Bo Liu, Li-Ming Zhan, Li Xu, Lin Ma, Yan Yang, and Xiao-Ming Wu. Slake: A semantically-labeled knowledge-enhanced dataset for medical visual question answering, 2021. URL <https://arxiv.org/abs/2102.09542>.

- Sahal Shaji Mullappilly, Mohammed Irfan Kurpath, Sara Pieri, Saeed Yahya Alseiari, Shanavas Cholakkal, Khaled Aldahmani, Fahad Khan, Rao Anwer, Salman Khan, Timothy Baldwin, et al. Bimedix2: Bio-medical expert lmm for diverse medical modalities. *arXiv preprint arXiv:2412.07769*, 2024.
- OpenAI. Introducing GPT-4.1 in the API. <https://openai.com/index/gpt-4-1/>, apr 2025.
- Vicente Ordonez, Girish Kulkarni, and Tamara Berg. Im2text: Describing images using 1 million captioned photographs. *Advances in neural information processing systems*, 24, 2011.
- Obioma Pelka, Sven Koitka, Johannes Rückert, Felix Nensa, and Christoph M. Friedrich. Radiology objects in context (ROCO): A multimodal image dataset. In Danaïl Stoyanov, Zeke Taylor, Simone Balocco, Raphael Sznitman, Anne L. Martel, Lena Maier-Hein, Luc Duong, Guillaume Zahnd, Stefanie Demirci, Shadi Albarqouni, Su-Lin Lee, Stefano Moriconi, Veronika Cheplygina, Diana Mateus, Emanuele Trucco, Eric Granger, and Pierre Jannin (eds.), *Intravascular Imaging and Computer Assisted Stenting - and - Large-Scale Annotation of Biomedical Data and Expert Label Synthesis - 7th Joint International Workshop, CVII-STENT 2018 and Third International Workshop, LABELS 2018, Held in Conjunction with MICCAI 2018, Granada, Spain, September 16, 2018, Proceedings*, volume 11043 of *Lecture Notes in Computer Science*, pp. 180–189. Springer, 2018. doi: 10.1007/978-3-030-01364-6_20. URL https://doi.org/10.1007/978-3-030-01364-6_20.
- Johannes Rückert, Louise Bloch, Raphael Brüngel, Ahmad Idrissi-Yaghir, Henning Schäfer, Cynthia S. Schmidt, Sven Koitka, Obioma Pelka, Asma Ben Abacha, Alba G. Seco de Herrera, Henning Müller, Peter A. Horn, Felix Nensa, and Christoph M. Friedrich. Rocov2: Radiology objects in context version 2, an updated multimodal image dataset. *Scientific Data*, 11(1), June 2024. ISSN 2052-4463. doi: 10.1038/s41597-024-03496-6. URL <http://dx.doi.org/10.1038/s41597-024-03496-6>.
- Andrew Sellergren, Sahar Kazemzadeh, Tiam Jaroensri, Atilla Kiraly, Madeleine Traverse, Timo Kohlberger, Shawn Xu, Fayaz Jamil, Cían Hughes, Charles Lau, et al. Medgemma technical report. *arXiv preprint arXiv:2507.05201*, 2025.
- Irene Siragusa, Salvatore Contino, Massimo La Ciura, Rosario Alicata, and Roberto Pirrone. Medpix 2.0: A comprehensive multimodal biomedical data set for advanced ai applications with retrieval augmented generation and knowledge graphs. *Data Science and Engineering*, July 2025. ISSN 2364-1541. doi: 10.1007/s41019-025-00297-8. URL <http://dx.doi.org/10.1007/s41019-025-00297-8>.
- Qiang Tang, Xian Liu, T. Kamins, G.S. Solomon, and J.S. Harris. Si nanowires growth catalyzed by tisi/sub 2/ islands in gas-source mbe. In *International Conference on Molecular Beam Epitaxy*, pp. 51–52, 2002. doi: 10.1109/MBE.2002.1037755.
- Kimi Team, Angang Du, Bohong Yin, Bowei Xing, Bowen Qu, Bowen Wang, Cheng Chen, Chenlin Zhang, Chenzhuang Du, Chu Wei, et al. Kimi-vl technical report. *arXiv preprint arXiv:2504.07491*, 2025a.
- LASA Team, Weiwen Xu, Hou Pong Chan, Long Li, Mahani Aljunied, Ruifeng Yuan, Jianyu Wang, Chenghao Xiao, Guizhen Chen, Chaoqun Liu, Zhaodonghui Li, Yu Sun, Junao Shen, Chaojun Wang, Jie Tan, Deli Zhao, Tingyang Xu, Hao Zhang, and Yu Rong. Lingshu: A generalist foundation model for unified multimodal medical understanding and reasoning, 2025b. URL <https://arxiv.org/abs/2506.07044>.
- Weizhi Wang, Khalil Mrini, Linjie Yang, Sateesh Kumar, Yu Tian, Xifeng Yan, and Heng Wang. Finetuned multimodal language models are high-quality image-text data filters. *arXiv preprint arXiv:2403.02677*, 2024.
- Weizhi Wang, Yu Tian, Linjie Yang, Heng Wang, and Xifeng Yan. Open-qwen2vl: Compute-efficient pre-training of fully-open multimodal llms on academic resources. *arXiv preprint arXiv:2504.00595*, 2025.

- Yunfei Xie, Ce Zhou, Lang Gao, Juncheng Wu, Xianhang Li, Hong-Yu Zhou, Sheng Liu, Lei Xing, James Zou, Cihang Xie, and Yuyin Zhou. Medtrinity-25m: A large-scale multimodal dataset with multigranular annotations for medicine. In *The Thirteenth International Conference on Learning Representations, ICLR 2025, Singapore, April 24-28, 2025*. OpenReview.net, 2025. URL <https://openreview.net/forum?id=IwgmgidYPS>.
- An Yang, Anfeng Li, Baosong Yang, Beichen Zhang, Binyuan Hui, Bo Zheng, Bowen Yu, Chang Gao, Chengen Huang, Chenxu Lv, Chujie Zheng, Dayiheng Liu, Fan Zhou, Fei Huang, Feng Hu, Hao Ge, Haoran Wei, Huan Lin, Jialong Tang, Jian Yang, Jianhong Tu, Jianwei Zhang, Jianxin Yang, Jiayi Yang, Jing Zhou, Jingren Zhou, Junyang Lin, Kai Dang, Keqin Bao, Kexin Yang, Le Yu, Lianghao Deng, Mei Li, Mingfeng Xue, Mingze Li, Pei Zhang, Peng Wang, Qin Zhu, Rui Men, Ruize Gao, Shixuan Liu, Shuang Luo, Tianhao Li, Tianyi Tang, Wenbiao Yin, Xingzhang Ren, Xinyu Wang, Xinyu Zhang, Xuancheng Ren, Yang Fan, Yang Su, Yichang Zhang, Yinger Zhang, Yu Wan, Yuqiong Liu, Zekun Wang, Zeyu Cui, Zhenru Zhang, Zhipeng Zhou, and Zihan Qiu. Qwen3 technical report, 2025. URL <https://arxiv.org/abs/2505.09388>.
- Linli Yao, Lei Li, Shuhuai Ren, Lean Wang, Yuanxin Liu, Xu Sun, and Lu Hou. Deco: Decoupling token compression from semantic abstraction in multimodal large language models, 2024. URL <https://arxiv.org/abs/2405.20985>.
- Xiang Yue, Yuansheng Ni, Kai Zhang, Tianyu Zheng, Ruoqi Liu, Ge Zhang, Samuel Stevens, Dongfu Jiang, Weiming Ren, Yuxuan Sun, et al. Mmmu: A massive multi-discipline multimodal understanding and reasoning benchmark for expert agi. In *Proceedings of the IEEE/CVF Conference on Computer Vision and Pattern Recognition*, pp. 9556–9567, 2024.
- Xiaoman Zhang, Chaoyi Wu, Ziheng Zhao, Weixiong Lin, Ya Zhang, Yanfeng Wang, and Weidi Xie. Pmc-vqa: Visual instruction tuning for medical visual question answering. *arXiv preprint arXiv:2305.10415*, 2023.
- Baichuan Zhou, Ying Hu, Xi Weng, Junlong Jia, Jie Luo, Xien Liu, Ji Wu, and Lei Huang. Tinyllava: A framework of small-scale large multimodal models. *arXiv preprint arXiv:2402.14289*, 2024.
- Jinguo Zhu, Weiyun Wang, Zhe Chen, Zhaoyang Liu, Shenglong Ye, Lixin Gu, Hao Tian, Yuchen Duan, Weijie Su, Jie Shao, et al. Internvl3: Exploring advanced training and test-time recipes for open-source multimodal models. *arXiv preprint arXiv:2504.10479*, 2025.
- Wanrong Zhu, Jack Hessel, Anas Awadalla, Samir Yitzhak Gadre, Jesse Dodge, Alex Fang, Youngjae Yu, Ludwig Schmidt, William Yang Wang, and Yejin Choi. Multimodal c4: An open, billion-scale corpus of images interleaved with text. *Advances in Neural Information Processing Systems*, 36:8958–8974, 2023.
- Yuxin Zuo, Shang Qu, Yifei Li, Zhangren Chen, Xuekai Zhu, Ermo Hua, Kaiyan Zhang, Ning Ding, and Bowen Zhou. Medxpertqa: Benchmarking expert-level medical reasoning and understanding. *arXiv preprint arXiv:2501.18362*, 2025.

A APPENDIX

A.1 THE USE OF LARGE LANGUAGE MODELS

We used large language models (LLMs) to check for grammatical inaccuracies and to improve the clarity and flow of the text. By helping to articulate the presented ideas more precisely, the use of LLMs contributed to enhancing the document’s readability.

A.2 SCORING GUIDELINES

This appendix provides the detailed scoring guidelines used to evaluate the quality of the sampled data across five dimensions: (1) Medical Information Accuracy, (2) Language Clarity and Fluency, (3) Dialogue Completeness, (4) Medical Imaging Relevance, and (5) Practicality. Each dimension is scored on a 1–5 scale, with higher scores indicating better quality. The guidelines were designed in collaboration with medical experts to ensure domain relevance and consistency.

Prompt for Quality Assessment

You are evaluating the quality of a single data sample from medical datasets, including three types: visual question answering, captioning, and case reporting. Rate the sample on a scale of 1 to 5 for each of the following five dimensions, and provide a clear explanation for your score. Your response must be in a valid JSON format, strictly following the structure below.

Evaluation Dimensions and Guidelines

1. Medical Information Accuracy: Definition: How medically accurate and clinically appropriate is the information in this sample? Evaluate whether the diagnosis, symptoms, treatment, terminology, and reasoning are factually correct and aligned with standard medical knowledge.

- 1 – Contains serious factual errors or misinformation; could lead to harm.
- 2 – Includes noticeable inaccuracies or misconceptions; questionable clinical logic.
- 3 – Mostly accurate, but includes some outdated, vague, or imprecise information.
- 4 – Clinically sound and reliable, with only minor wording or factual issues.
- 5 – Fully medically accurate, consistent with guidelines and expert-level clarity.

2. Language Clarity and Fluency: Definition: How well is the information communicated in natural, readable, and professional language? Assess grammar, clarity, flow, and appropriateness for medical or patient-facing communication.

- 1 – Unclear or disorganized; major grammar issues that hinder understanding.
- 2 – Awkward, ambiguous, or frequently incorrect language.
- 3 – Understandable but with some unnatural phrasing or awkward sentence structure.
- 4 – Clear and coherent; only minor language flaws.
- 5 – Highly fluent, polished, and well-suited for clinical or academic contexts.

3. Caption/Dialogue Completeness: Definition: For multi-turn dialogue, does the exchange include all key components of a meaningful clinical interaction (e.g., symptoms, history, reasoning, advice)? Evaluate whether the conversation flows logically and covers necessary content. For single-turn samples or caption, assess whether the response directly, sufficiently, and contextually addresses the input question or concern.

- 1 – Severely incomplete or off-topic; the response fails to address the input meaningfully.
- 2 – Major gaps; the response is only partially relevant or lacks necessary context.
- 3 – Generally appropriate, but missing some useful clarifications or elaboration.
- 4 – Mostly complete; clear and contextually suitable with minor detail omissions.
- 5 – Fully complete and coherent; the response provides an informative and context-aware answer, proportional to the input.

Note: For multi-turn dialogue, completeness includes aspects like logical progression, topic coverage, and closure. For single-turn Q&A, completeness means answering the question clearly, relevantly, and with appropriate medical insight.

4. Medical Imaging Relevance: Definition: If an image is present, does it clearly support or correspond to the associated text? Judge how well the image reinforces or illustrates the medical concepts being discussed.

- 1 – No image provided, or image is irrelevant/inappropriate. (Assign 1 by default if no image.)
- 2 – Weak connection; image adds little or may be confusing.
- 3 – Somewhat related; offers limited value or context.
- 4 – Relevant and supports the written content effectively.
- 5 – Strong alignment between image and text; image enhances understanding.

Note: If no image is provided in the sample, write: "No image provided. Assigning a score of 1 by default." and assign score = 1

5. Practicality: Definition: How useful is this data sample for real-world medical applications? Consider utility in model training, clinical decision support, educational value, or real patient interaction systems.

- 1 – No practical use; irrelevant or flawed content.
- 2 – Very limited applicability in specialized cases only.
- 3 – Somewhat useful; suitable for non-critical training or analysis.
- 4 – Practical and usable with minor improvements.
- 5 – Highly valuable for real-world use; clinically or technically actionable.

Overall Score Definition: Based on your evaluation across all five dimensions, assign a final overall score that reflects the holistic quality of the data sample. Consider accuracy, clarity, completeness, image relevance (if applicable), and practical usability as a whole. This score is not necessarily the average, but should represent your expert judgment of the sample’s real-world value.

- 1 – Very poor overall; unreliable, misleading, or unusable.
- 2 – Weak quality; flawed in multiple aspects, limited usability.
- 3 – Adequate; some issues, but can be useful in certain contexts.
- 4 – Good quality; mostly solid with minor areas for improvement.
- 5 – Excellent; reliable, polished, and ready for real-world use or modeling.

The response format is:

```
{
  "Medical Information Accuracy": {"score": <1-5>,
  "comment": "<explanation>"},
  "Language Clarity and Fluency": {"score": <1-5>, "comment": "<explanation>"},
  "Dialogue Completeness": {"score": <1-5>, "comment": "<explanation>"},
  "Medical Imaging Relevance": {"score": <1-5>, "comment": "<explanation>"},
  "Practicality": {"score": <1-5>, "comment": "<explanation>"},
  "Overall": {"score": <1-5>, "comment": "<summary comment>"}
}
```

Here is the sample: {s}

A.3 DATA MIXING DETAILS

The training pipeline employs a structured four-stage data mixture strategy to progressively build the model’s capabilities, as detailed in Table 4.

The process begins with continual pretraining on a large-scale foundation of both general-domain multimodal data (e.g., DataComp, OBELICS) and extensive medical caption data (e.g., Medtrinity-25M, ROCO), totaling approximately 30 billion tokens. This stage aims to establish robust visual and linguistic representations.

Next, the model’s instruction-following ability is honed in two distinct phases. First, general instruction following is trained exclusively on the Mammoth-VL-10M dataset (~10.1M samples). This is followed by medical instruction following, which combines a filtered portion of Mammoth-VL-10M with multiple medical instruction datasets (e.g., Path-VQA, PMC-VQA), resulting in a mixture of ~11.69M samples.

Finally, for cross-distribution instruction adaption, the data is subsampled to create a balanced and high-quality mixture. This stage uses a small, curated set of ~304k samples, comprising 180K from Mammoth-VL-10M and a balanced blend from key medical instruction datasets (e.g., 13K from LLaVA-Med-Instruct, 20K from PMC-VQA).

Table 4: The overview of the data mixture across the four training stages. Noted that mammoth-VL-10M-filtered variant excludes safety refusal responses (e.g., "Sorry, I can't..."), and #number denotes the number of samples after downsampling.

Stage	Training Data Composition	Amount
Continual Pretraining	1. General Multimodal Data DataComp, CCS, OBELICS, mmc4 2. Medical Caption Data LLaVA-Med-60K-IM-Text, LLaVA-Med-Alignment, LLaVA-Med-Fig-Caption, Medtrinity-25M, PubMedVision-Alignment, ROCO-radiology, ROCov2-radiology Mammoth-VL-10M	~ 30B tokens
General Instruction Following	Mammoth-VL-10M	~ 10.1M samples
Medical Instruction Following	1. General Instruction Data Mammoth-VL-10M-filtered 2. Medical Instruction Data LLaVA-Med-Instruct, Path-VQA, PMC-VQA, PubMedVision-Instruct Tuning, SLAKE, VQA-RAD	~11.69M samples
Cross-Distribution Instruction Adaptation	1. Sampled General Instruction Data Mammoth-VL-10M-filtered#180K 2. Sampled Medical Instruction Data LLaVA-Med-Instruct#13K, Path-VQA, PMC-VQA#20K, PubMedVision-Instruct Tuning#60K, SLAKE, VQA-RAD	~ 304K samples

Table 5: Implementation details and hyperparameters for InfiMed-Foundation pretraining and supervised fine-tuning.

Details	Pretraining	SFT
Vision Encoder	SigLIP-so400m-384px	SigLIP-so400m-384px
Visual Projector	Adaptive Average Pooling + MLP	MLP
LLM	Qwen3-1.7B-Instruct / Qwen3-4B-Instruct	Qwen3-1.7B-Instruct / Qwen3-4B-Instruct
Tokens per Image	144	729
Context Length	4096	4096
Sequence Packing	Yes	No
Global Batch Size	256	128
Training Epoch	1	1 per stage
Optimizer	AdamW	AdamW
Peak LR	5e-5	2e-5
Warmup Ratio	3%	3%
Weight Decay	0.01	0.01

A.4 EVALUATION FRAMEWORK

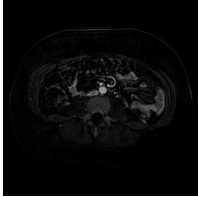
To improve the efficiency and fairness of the evaluation, we adopt the MedEvalKit evaluation framework (Team et al., 2025b). This framework is designed to support a comprehensive set of mainstream medical benchmarks. MedEvalKit employs a standardized data preprocessing and postprocessing pipeline to ensure consistency and comparability of results. The framework implements a rule-based evaluation approach for closed-ended questions, which provides precise and objective scoring based on predefined criteria. For open-ended questions, MedEvalKit leverages an LLM-as-a-Judge strategy, utilizing advanced language models to assess response quality. Furthermore, the framework integrates vLLM (Kwon et al., 2023) for inference acceleration, significantly improving computational efficiency and scalability.

A.5 IMPLEMENTATION DETAILS

The implementation details and hyperparameters for InfiMed-Foundation model pretraining and SFT are presented in Table 5. We used Qwen3-1.7B-Instruct and Qwen3-4B-Instruct as the large language model (LLM) backbones, and SigLIP as the vision transformer (ViT) backbone. The LLM input length is truncated at 4096 tokens. For pretraining, we utilized 32 NVIDIA H800 (80GB) GPUs. The optimizer is AdamW with a learning rate of 5e-5, weight decay of 0.01, and a warmup ratio of 0.03. The pretrain global batch size is 256. We pretrain the MLLM for one epoch. For supervised fine-tuning (SFT), we used 16 GPUs. The optimizer remains AdamW, but with a learning rate of 2e-5, a larger weight decay of 0.1, and the same warmup ratio of 0.03. The SFT global batch size is set to 128. Each stage of SFT is trained for one epoch.

A.6 CASE STUDY

This section presents a series of case studies comparing the responses of Qwen2.5-VL-7B and our InfiMed-Foundation-4B model. Through qualitative analysis of specific examples, we demonstrate that InfiMed-Foundation-4B, despite its smaller size, exhibits a more solid grasp of medical knowledge, providing more accurate and reliable answers than its larger counterpart.



Question:
What modality was used to obtain this image capture?
A: CT scan B: Ultrasound C: MRI D: Echocardiogram

Ground Truth:
C: MRI

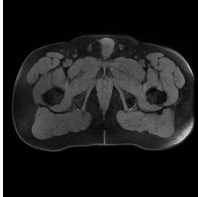
Qwen2.5-VL-7B Answer:

⊘ The image appears to be a cross-sectional view of the abdomen, which is characteristic of a CT scan. The high contrast and the ability to visualize internal structures in detail are typical of CT imaging. Ultrasound images are usually in grayscale and show different textures, MRI images often have a different contrast pattern, and echocardiograms are used for heart imaging. (A. CT scan)

InfiMed-Foundation-4B Answer:

😊 The image provided is a cross-sectional view of the abdomen, showing various internal structures such as the liver, kidneys, and intestines. The image has a high level of detail and contrast, which is characteristic of certain imaging modalities. Let's analyze the options: A. CT scan: CT scans use X-rays to create detailed images of the body. They often have a high level of detail and contrast, but the image provided does not have the typical appearance of a CT scan. B. Ultrasound: Ultrasound images are typically grainy and have a different appearance due to the use of sound waves. The image provided does not match this description. C. MRI: MRI uses strong magnetic fields and radio waves to create detailed images of the body. MRI images often have high contrast and can show soft tissues in great detail, which matches the characteristics of the provided image. D. Echocardiogram: Echocardiograms are used to visualize the heart and blood vessels. They typically produce images of the heart and do not show abdominal structures. Based on the analysis, the most likely modality used to obtain this image is MRI. Final Answer: (C)

Figure 4: Case study No.1: Qwen2.5-VL-7B vs. InfiMed-Foundation-4B on Medical VQA.



Question:
Is the image showing any indication of abnormality?
A: It's difficult to determine if there is an abnormality based on this image.
B: I'm not sure, but there might be a slight abnormality.
C: No, It's normal.
D: There is a possibility of abnormality, but further tests are needed for confirmation.

Ground Truth:
C. No, It's normal.

Qwen2.5-VL-7B Answer:

⊘ The image appears to be a medical scan, likely an MRI or CT scan, showing a cross-section of the body. The structures within the scan are not clearly identifiable without medical expertise, but there are no obvious signs of abnormality such as masses, irregularities, or asymmetry that would immediately suggest a problem. However, a definitive assessment requires a professional medical interpretation. (A. It's difficult to determine if there is an abnormality based on this image.)

InfiMed-Foundation-4B Answer:

😊 To determine if there is an indication of abnormality in the image, we need to carefully analyze the structures and compare them to normal anatomy. The image appears to be an MRI scan of the pelvic region, showing the symmetrical appearance of the hip bones, muscles, and surrounding tissues. Symmetry: The image shows a symmetrical appearance of the hip bones and surrounding muscles, which is generally a good sign. Muscle and tissue integrity: The muscles and tissues appear to be intact without any obvious signs of damage or irregularities. No visible masses or lesions: There are no visible masses, lesions, or abnormal growths in the image. Based on these observations, it seems that the image does not show any indication of abnormality. Therefore, the most appropriate answer is: (C. No, It's normal.)

Figure 5: Case study No.2: Qwen2.5-VL-7B vs. InfiMed-Foundation-4B on Medical VQA. Qwen2.5-VL-7B was unable to make a judgment due to a lack of medical knowledge.



Question:
Is the anomaly observed in this image benign or malignant?
A: Benign image.
B: Malignant

Ground Truth:
A: Benign image.

Qwen2.5-VL-7B Answer:

☹️ <think>\nThe image shows a skin lesion with irregular borders and a slightly elevated surface, which are characteristics often associated with malignant melanomas. The presence of a ruler for scale suggests the lesion is larger than 6mm, which is a significant size for a mole that should be evaluated by a dermatologist. However, without professional medical evaluation, it's not possible to definitively determine the nature of the lesion.\n</think>\n\boxed{B. Malignant}

InfiMed-Foundation-4B Answer:

😊 The reasoning process is as follows:\n\n1. The image shows a skin lesion with a brownish color and a slightly irregular shape.\n2. The lesion appears to be a mole or a nevus, which is a common type of skin growth.\n3. The color and shape of the lesion are important factors in determining whether it is benign or malignant.\n4. Benign moles typically have a uniform color and shape, while malignant moles may have an irregular shape, uneven color, and a raised or pitted surface.\n5. Based on the image, the lesion appears to have a relatively uniform color and shape, which suggests that it is likely benign.\n\nTherefore, the most likely answer is:\n\nA. Benign image."

Figure 6: Case study No.3: Qwen2.5-VL-7B vs. InfiMed-Foundation-4B on Medical VQA. Qwen2.5-VL-7B made an incorrect estimation of the lesion size.



Question:
Is there any indication of abnormality that can be observed in this image?
A: Yes B: No

Ground Truth:
B: No

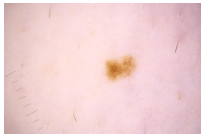
Qwen2.5-VL-7B Answer:

☹️ <think>\nThe image appears to be a CT scan of the chest. There is a large, well-defined mass in the right upper lobe of the lung, which is not typical for a normal lung. This could be indicative of a pathological condition such as a tumor or a mass lesion. However, a definitive diagnosis would require clinical correlation and further imaging or biopsy.\n</think>\n\boxed{A. Yes.}

InfiMed-Foundation-4B Answer:

😊 The image provided is a CT scan of the chest, showing the heart, lungs, and surrounding structures. To determine if there are any indications of abnormality, we need to carefully examine the key features in the image.\n\n1. **Heart**: The heart appears to be of normal size and shape. There are no visible signs of enlargement or abnormal contours.\n2. **Lungs**: The lungs are clear, with no evidence of masses, nodules, or areas of consolidation. The lung fields are well-aerated.\n3. **Major Blood Vessels**: The aorta and pulmonary arteries appear normal in size and shape.\n4. **Bones**: The ribs and vertebrae are intact, with no signs of fractures or lesions.\n5. **Soft Tissues**: There are no abnormal masses or fluid collections in the soft tissues surrounding the chest.\n\nGiven this detailed examination, there are no indications of abnormality in the image.\n\nFinal Answer: \boxed{B. No}

Figure 7: Case study No.4: Qwen2.5-VL-7B vs. InfiMed-Foundation-4B on Medical VQA. Qwen2.5-VL-7B produced an erroneous judgment, whereas InfiMed-Foundation-4B conducted a systematic analysis.



Question:
What modality was used to obtain this image capture? Is the abnormality in this image a benign or malignant image?

A: Malignant B: Benign image

Ground Truth:
B: Benign image

Qwen2.5-VL-7B Answer:

 <think>\n\nThe image shows a brownish spot on a light-colored surface, which could be indicative of a mole or a skin lesion. However, without professional medical evaluation, it's not possible to determine if this is benign or malignant. The appearance could be consistent with a variety of skin conditions, including benign moles or potentially more serious issues like melanoma. A dermatologist's examination is necessary for a definitive diagnosis.\n/</think>\n\nboxed{A. Malignant}

InfiMed-Foundation-4B Answer:

 The image depicts a skin lesion that appears to be a mole or a similar type of skin marking. To determine whether it is benign or malignant, we need to consider several factors such as its size, shape, color, and borders. \n\n1. **Size**: The lesion appears to be relatively small, which is often a characteristic of benign moles. \n2. **Shape**: The shape of the lesion is somewhat irregular but not extremely so, which can sometimes be seen in benign moles. \n3. **Color**: The lesion has a uniform brown color, which is common in benign moles. \n4. **Borders**: The borders of the lesion appear to be well-defined, which is another characteristic often seen in benign moles. \n\nGiven these observations, the lesion seems to have features that are more consistent with a benign mole rather than a malignant one. Therefore, the most likely classification for this lesion is:\n\nSimple Answer: B

Figure 8: Case study No.5: Qwen2.5-VL-7B vs. InfiMed-Foundation-4B on Medical VQA. Qwen2.5-VL-7B exhibits a deficiency in medical knowledge.